VARIABILITY OF REGULAR RELIEF CELLS FORMED ON COMPLEX FUNCTIONAL SURFACES BY SIMULTANEOUS FIVE-AXIS BALL BURNISHING

Stoyan SLAVOV[1], Diyan DIMITROV[2], Iliyan ILIEV[3]

The present work describes experimentally obtained results for the shape and size variability of the cells from regular reliefs, obtained by simultaneous five-axis ball-burnishing process on complex surfaces, performed on multi-axis CNC milling center. An experiment to determine the influence of the main ball burnishing regime parameters is carried out. The methodologies of the conducted experiment and the measurements are described, and the obtained results are illustrated and discussed. As a result it is found that more significant of the examined parameters of the cells size and shape variability are the ones, related to the characteristics of the deforming element toolpath (frequency and amplitude) than the other parameters, which refer to the plastic deformation (force and ball tool diameter).

Keywords: Five-axis simultaneous machining; Ball burnishing; ANOVA; Pareto

1. Introduction

Conventional burnishing and deep rolling finishing operations are often used, when smooth surface finish (near to mirror surface) must be obtained, or the surface layer must be hardened and compressive residual stresses must be formed on it [1]. Unlike some other finishing processes [2,3], burnishing and deep rolling are based on cold plastic deformation in the surface layer, which is obtained as a result of the impact of the passing deforming element(s) (which can be hardened steel balls, rollers or diamond inserts) pressed with a certain force into the processed surface (see Fig. 1, a). Different types of outer and inner cylindrical or tapered parts, and also planar or even complex (spherical, hyperbolic, etc.) surfaces can be burnished, using these finish methods [1,4]. There is a wide choice of standardized ball, roller or diamond burnishing tools, which are designed to work with both conventional (manually operated) and CNC lathe or milling machines [5,6]. The kinematics of the classic machine tools, along with the finish canned cycles and the strategies, integrated in CNC machines are suitable to perform almost all classic

[1] Assoc. prof., Dept. of Mechanical Engineering and Machine Tools, Technical University of Varna, Bulgaria, e-mail: sdslavov@tu-varna.bg
[2] Assoc. prof., Dept. of Mechanics and Machine Elements, Technical University of Varna, Bulgaria, e-mail: dm_dimitrov@tu-varna.bg
[3] PHD student, Dept. of Mechanical Engineering and Machine Tools, Technical University of Varna, Bulgaria, e-mail: iliyan.iliev@tu-varna.bg

burnishing operations, since they can provide the needed toolpaths, which are the same as those, used in cutting operations. Only regime parameters, such as spindle speeds and feedrate are different in cutting and burnishing operations.

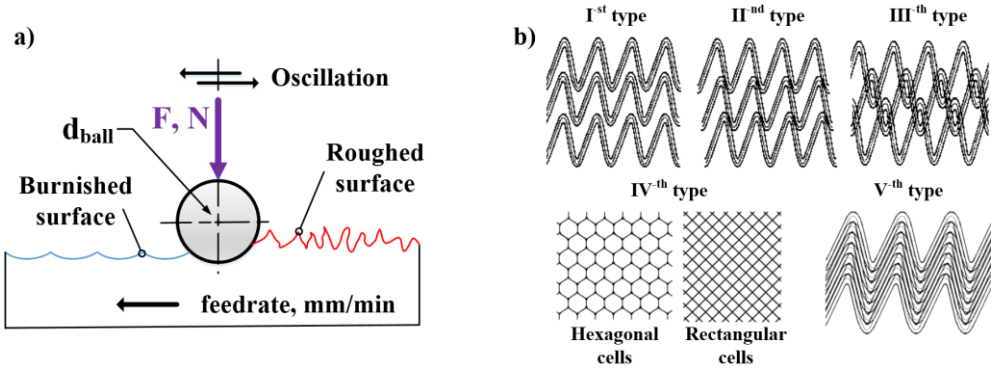

Fig. 1. a) Diagram of vibratory ball burnishing process; b) Classification of the regular reliefs, obtained after vibratory ball burnishing.

Sometimes the ball burnishing (BB) process is also used to form a specific analytically calculable roughness onto the burnished surface in addition to the improvement of its physical and mechanical characteristics [4,7]. For that purpose, an additional oscillation of the ball tool (with a certain frequency and amplitude), in parallel to the processed surface direction, is added to the classic burnishing operation (see Fig. 1. a). As a result of the correlation between the oscillations of the burnishing tool and the other BB regime parameters, the plastically deformed traces, obtained after the ball deforming element passage, create the so-called "partially" or "completely" regular reliefs (RR) of types, shown in the Fig. 1, b). These RR are classified into five different types [7]. The first three types being meshes of non-contacting, tangenting or intersecting deformed traces. They are called "partially" RR because they do not completely cover the burnished surface. The IV-th and V-th types RR completely cover the whole burnished surface, and they do not contain "islands" with remnant roughness from the cutting operation, preceding the burnishing operation. When a IV-th type RR is processed, specific rectangular or hexagonal cell patterns are formed, whose shape and size depend on the pre-set BB regime parameters, unlike the V-th type RR, in which no cells are formed.

Various schemes, based on manually operated machine tools (MOMT) are developed in order to form RR onto cylindrical (see Fig. 2, a) or planar (see Fig. 2, b) surfaces by BB [1,4,7]. They usually include specially constructed vibration assisted burnishing tools in order to achieve the required, close to sinusoidal toolpath of the deforming element. As a result, the obtained RR's cells of the IV-th type have a comparatively good uniformity in terms of shape and size all over the burnished surface, which mainly depends on the BB process parameters stability during the operation.

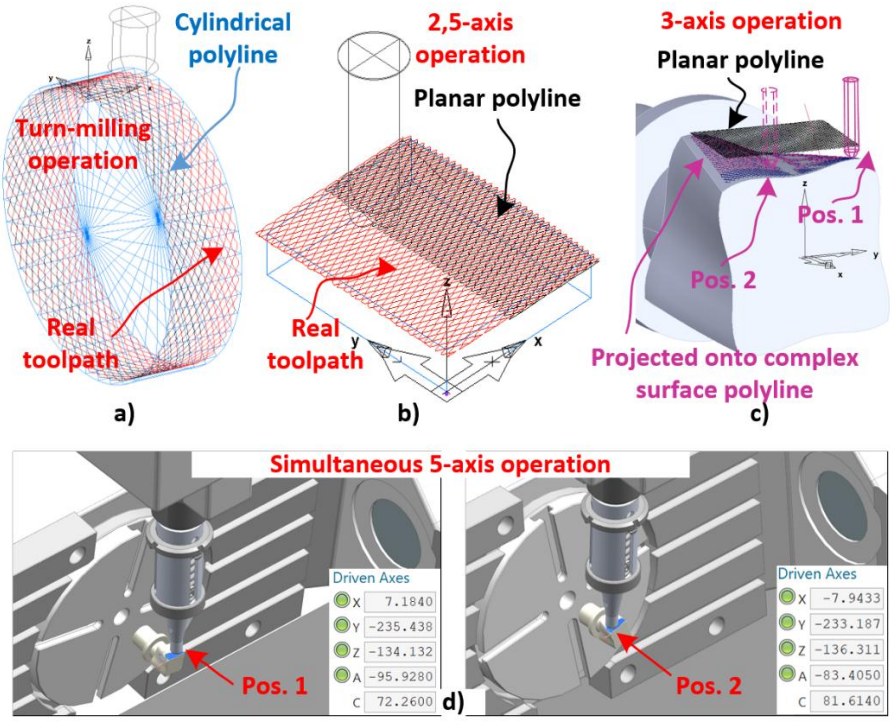

Fig. 2. Different deforming tool trajectories to form RR of the IV-th type by BB process for different types of functional surfaces: a) cylindrical; b) planar, c) and d) with free-form shape.

The use of MOMT, however, to obtain RR of the IV-th type has several important limitations. For example, many of the BB regime parameters cannot be set continuously, when using MOMT, often there is no precise synchronization between the machine's actuators, some of the BB regime parameters can fluctuate slightly during the operation, etc. This results in obtaining RR of different cell shapes and sizes. Furthermore, the classical MOMT cannot provide the needed sinusoidal toolpath of the deforming ball, and they have limited capabilities with regard to burnishing complex surfaces. If CNC-machines, in combination with suitable CAD-CAM software, are used instead of MOMT, it is possible to avoid most of the aforementioned drawbacks [8-18]. The contemporary CNC lathe and milling centers are able to perform burnishing operations without any forced vibrations and all five types of RR can be formed onto cylindrical, planar, or even complex surfaces (see Fig. 2, a-c), such as turbine blades, marine propellers, compressors, etc. They have greater accuracy [19, 20], productivity, and can operate in a simultaneous multi-axis mode [21], in comparison to many of the classic MOMT.

Unfortunately, the contemporary CAMs and CNCs machine tools do not integrate specially developed cycles (or operations) for RR processing. However, almost all of them support operations, in which the tip of the tool can be guided by a predefined planar or spatial curve(s). An appropriate (complex) toolpath curve (or

polyline), generated in CAD can be imported and used in CAM to define the needed complex toolpath of the deforming tool and to create a numerical code.

If the burnished surfaces have a cylindrical or a planar shape (see Fig. 2, a, b) the generation and positioning of toolpath curves over the processed surfaces are relatively simple tasks, but when the surface has a non-planar shape (see Fig. 2, c), it is much more difficult. An approach, based on the projection of the generated 2D polyline onto a non-planar surface, is described in [14]. Then this projected nonplanar curve is used as a toolpath in the BB operation. In 3-axis milling operations, the axis of the tool will always be parallel to the Z axis of the machine, and it will not coincide with the normal vector of the machined surface at the point of contact. This is undesirable, since it will lead to variability in the deforming force and hence the different physical and mechanical characteristics of the resulting RR in different areas of the processed surface. For this reason, it is necessary to use a simultaneous 5-axis milling operation when processing nonplanar surfaces of a complex shape. The used CAM's features (or such operations) must allow the tip of the burnishing tool to be guided along the projected 3D polyline (i.e. toolpath), and to continuously tilt its axis at the same time, so that it is always perpendicular to the local curvature of the processed complex surface (see Fig. 2, d and Fig. 3, c).

However, projecting the 2D polyline onto the nonplanar surface (see Fig 2, c) can lead to some deformation of the RR cell's shape and size, which will depend on the 3D topography of the processed complex surface. The larger the curvature of the surface, the greater the deformations will be. The 5-axis operation algorithm abilities of the CAM software, the used multi-axis postprocessor for generating NC code, and the algorithms for multi-axis interpolation, integrated in the CNC of the machine tool, also have an effect on these deformations. They cannot be verified only by using 3D simulations, since the simulation in CAM software is not intended to model resulting plastic deformations in the surface layer.

Source [22] describes an attempt for determining the RR's cells irregularity after 5-axis BB. The longitudinal and transverse steps of the RR's cells, as well as the angle between them and the diameter of the circles, inscribed within the boundaries of the cells, are measured. Unfortunately, the measurements have been conducted at the normal position of the microscope lens relative to the complex lateral surface of the specimens, which does not guarantee an accurate cell size determination. In addition, the author measures two steps and the diameter of the inscribed circle five times for each side of each specimen. However, the diameter itself could be used as a sufficient feature, determining the size of the cells. In this way, the number of measurements and the processing of the results could be reduced by half.

For these reasons, the main objectives of the present work are to determine experimentally the variability of the RR's cells shape and size, formed on complex surfaces and the influence of some important BB's regime parameters on this variability. An advanced measuring setup that allows more precise adjustment of

the microscope lens over the measured surface will be used in the experiments, and also up to two RR cells' parameters which describe sufficiently their shape and size.

2. Methodology of the experimental study

2.1. 5-axis BB operation setup description and experimental study design

To carry out the simultaneous five-axis BB operations, a CNC milling center HAAS VF-4, equipped with dual axis rotary table HAAS TR-110, and a specially designed ball deforming tool [23] are used (see Fig. 2, d and Fig. 3, c, e). The specimens (see Fig. 3, a, d) are made of Al-alloy 2024-T3 (BDS EN 754-3:2008). They have four sides with the same complex shape and dimensions, according to the diagram, shown on Fig. 3, a). The side surfaces are designed to have a shape, similar to that of the functional surfaces of the considered parts. The BB finishing operation is configured, using the CAM module of the Siemens NX software, and the corresponding NC programs are generated.

Full factorial experimental design with four factors at two levels per factor of type 2^4 [24] is conducted, to study the shape and size variability of the RR's cells. Every experimental run has four replications (see Table 2), which correspond to four nonplanar specimen's surfaces (see Fig. 3, a). The replications are used in the further conducted ANOVA analysis.

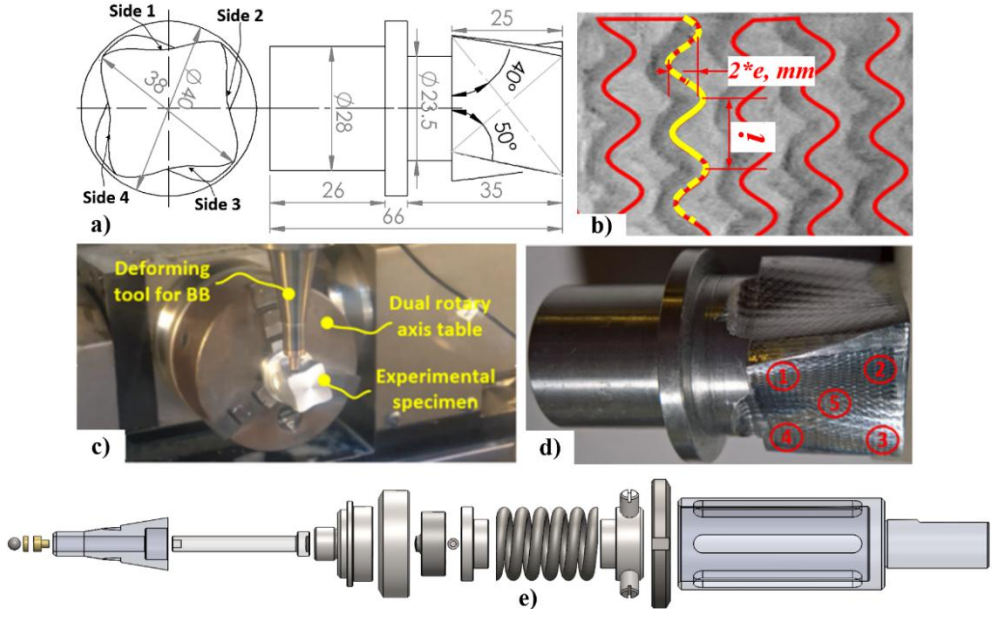

Fig. 3. a) Dimensions of the experimental specimens; b) Diagram of the BB regime parameters *e*, mm, and *i*; c) The five-axis BB operations on CNC milling center; d) BB specimen with formed RR of the IV-th type on side nonplanar surfaces by 5-axis BB process; e) Ball deforming tool [23].

In the current experiment, the main regime parameters of the BB process, which might have a significant effect on the shape and size of the resulting RR's cells, are chosen to be:

- ***d_b, mm*** – the diameter of the deforming ball-tool with high hardness (which is actually a ball from a ball bearing with an appropriate diameter);
- ***F, N*** – the pre-set (nominal) deforming force, applied to the deforming element by the spring of the tool;
- ***e, mm*** (see Fig. 3, b)– the pre-set amplitude of the sinusoidal trajectory, on which the tip of the deforming tool moves. This regime parameter defines the size of the RR's cells in horizontal direction;
- ***i*** (see Fig. 3, b) –the pre-set number of the sine waves, within the whole length of the toolpath. This regime parameter defines the length of the period of the sine waves (frequency) from the motion trajectory and hence the size of the RR's cells in vertical direction.

All experimental design combinations of the values in encoded and in real mode of the BB process regime parameters are shown in Table 1.

Table 1.

Full factorial experimental design of the type 2^4

№	Full factorial experiment – encoded values				Full factorial experiment – real values			
	d_b	***F***	***e***	***i***	***d_b, mm***	***F, N***	***e, mm***	***i***
1	-1	-1	-1	-1	6	250	0.5	1650.15
2	-1	-1	-1	1	6	250	0.5	2500.15
3	-1	-1	1	-1	6	250	1	1650.15
4	-1	-1	1	1	6	250	1	2500.15
5	-1	1	-1	-1	6	380	0.5	1650.15
6	-1	1	-1	1	6	380	0.5	2500.15
7	-1	1	1	-1	6	380	1	1650.15
8	-1	1	1	1	6	380	1	2500.15
9	1	-1	-1	-1	8	250	0.5	1650.15
10	1	-1	-1	1	8	250	0.5	2500.15
11	1	-1	1	-1	8	250	1	1650.15
12	1	-1	1	1	8	250	1	2500.15
13	1	1	-1	-1	8	380	0.5	1650.15
14	1	1	-1	1	8	380	0.5	2500.15
15	1	1	1	-1	8	380	1	1650.15
16	1	1	1	1	8	380	1	2500.15

The VF-4 milling center spindle is locked (using M19) during all BB operations, and the inverse time feed mode (command G93) is activated in the settings of the 5-axis postprocessor, when NC-code is generated.

Some of other BB process regime parameters, which can affect the resulting RR characteristics, such as the feed rate of the ball tool, the type of the lubricant used and the lubrication conditions, the prior roughness from previous machining operation, etc., do not participate as factors in the current experiment. The exclusion

of the feed rate parameter from the influencing factors of the experiment is due to the chosen synchronization mode of the five axes of the milling machine. In order to obtain a smoother tool trajectory for simultaneous multi-axis machining, it is advisable not to use a feed rate per minute (G94), but an inverse time feed mode (command G93 activated) [21]. In this G93 mode, the CAM 5-axis postprocessor generates a NC-code by calculating a different feed rate for each individual move of the tool between every two consecutive points of the tool path. In inverse time feed rate mode, an F word in NC-code means that the move should be completed in (1/F number) minutes. When the inverse time feed rate mode is active, an F word appears on every line, which has a G01, G02, or G03 motion command. Therefore, in present BB-operations it is impossible to "fix" the feed rate values only at "high" or "low" level for different factors levels combinations in the experimental design. That is why the feed rate is excluded as a factor in the current design of experiment.

In the present experimental study, the same type of lubricant (Mobil DTE 25) is used for all the 16 specimens, in order to avoid jamming of the ball tool. Before performing the finishing BB operations, the lateral nonplanar surfaces of all specimens (see Fig. 3, a) are previously machined by 3-axis rough and finish milling operations, which produced macroform of a nonplanar shape on side surfaces with surface roughness Rz up to 4.21 μm.

2.2. Methodology for RR's cells shape and size variability determination

The RR cells' shape measurement setup is shown on Fig. 4, a. The specimen (pos. 2) is hold in the chuck (pos. 3) of the indexing head (pos. 4). In this way its side nonplanar surfaces can be adjusted to be positioned as perpendicularly as possible to the axis of the microscope lens (pos. 1) for each of the five measured surface areas (see Fig. 4, c). Images with high resolution (12 MPix) of RR's cells are captured by using a DigiMicro Lab 5.0+ digital microscope, and then processed in dedicated measuring software, which allows precise measurements of the RR's cells geometry parameters.

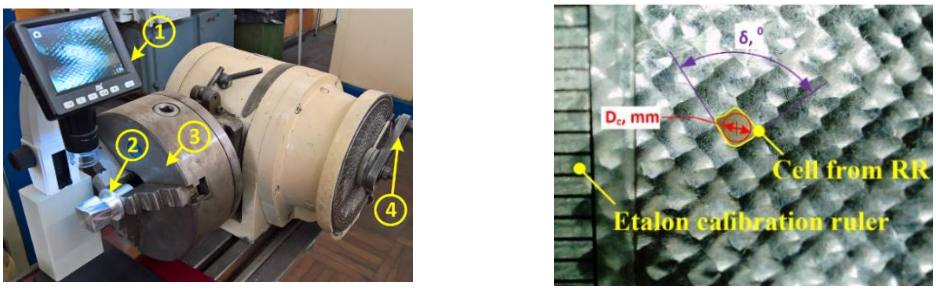

a) b)

Fig. 4. a) Setup for capturing high resolution images of RR; b) Digital image of RR's cells with indicated geometrical parameters for size – Dc, mm and for shape - δ,^{0} to be measured.

Before measuring the RR's cells parameters, every captured image is calibrated, using the etalon calibration ruler, in accordance with the manufacturer's calibration methodology. As a result, the corresponding magnification factor is calculated and then it is used to adjust the measured distances and to calculate their values with an accuracy up to 0.01 mm.

Using the above described methodology, 16×4×5=320 digital images (of the type shown in Fig. 4, b) are captured. They are used to measure the dimensions: *Dc*, mm (or the diameter of the inscribed circle within the cell) and $\delta,^0$ (or the angle enclosed between two adjacent cell boundaries) of the RR's cells. In order to determine the variability of the cells size and shape, measurements are made in five different areas on each side (see Fig. 3, d). Then for the measured five values for *Dc*, mm and for $\delta,^0$ for each of the five areas, the standard deviation (σ) and the mean ($\bar{X}$) values are calculated. Now, it is possible to calculate *CV* (or Coefficient of Variation) [25] by the following formula:

$$CV = \left(\sigma/\overline{X}\right) \cdot 100, \% \quad (1)$$

The parameter *CV* is used as a quantitative assessment criterion for the variability of RR's cells size and shape within the boundaries of every specimen's side nonplanar surface.

3. Processing the experimental results

The obtained values of the CVs for RR's cells geometrical parameters *Dc*, mm and $\delta,^0$ are shown in Table 2.

Table 2

Calculated CV values for RR size and shape parameters *Dc* and *δ*

№	Experimental results for the diameter of the inscribed circle - Dc				Experimental results for the angle enclosed between two adjacent cell boundaries - *δ*			
	CV, % (Side 1)	CV, % (Side 2)	CV, % (Side 3)	CV, % (Side 4)	CV, % (Side 1)	CV, % (Side 2)	CV, % (Side 3)	CV, % (Side 4)
1	4.518	1.363	4.392	2.020	4.487	3.371	3.556	2.921
2	4.753	1.850	4.536	3.804	0.356	3.408	5.755	2.121
3	3.209	2.809	4.863	2.362	7.261	1.985	4.172	2.799
4	6.369	2.969	5.094	3.241	7.388	6.130	7.282	6.557
5	6.588	7.148	2.905	6.454	5.514	5.424	3.672	2.219
6	6.065	6.357	3.226	6.272	3.071	5.042	5.438	4.960
7	1.041	5.168	2.939	0.936	6.759	0.780	5.884	2.028
8	3.499	6.414	6.061	3.827	6.267	3.078	4.275	3.726
9	3.340	1.863	2.080	5.388	3.966	2.037	2.642	3.459
10	1.775	4.793	3.987	2.967	6.282	2.471	3.428	5.785
11	4.284	5.656	3.753	4.667	1.180	3.175	2.062	5.500
12	6.061	3.413	2.156	5.980	5.207	5.947	6.275	6.661
13	2.598	4.141	5.441	2.716	3.429	5.612	4.470	2.166
14	5.082	5.257	6.934	6.165	5.461	3.596	6.451	4.084
15	1.109	1.773	4.796	2.728	6.840	4.639	5.496	3.989
16	5.250	3.393	4.337	3.704	4.451	7.832	3.544	6.827

In order to investigate the effects of the BB main regime parameters, the means CV_{low} and CV_{high} are calculated, using the following equations [25]:

$$\overline{CV}_{low} = \frac{1}{8} \cdot \left(\sum_{i=1}^{8} CV_i^{low}\right), \quad \overline{CV}_{high} = \frac{1}{8} \cdot \left(\sum_{i=9}^{16} CV_i^{high}\right) \tag{2}$$

where:

- CV_i^{low} – are those eight results from Table 2, where the regime parameters have low level values;
- CV_i^{high} – the other eight results, where the parameters have high level values.

The effect of each of the four BB process regime parameters d_b, F, e and i on the RR's cells size and shape variability is calculated by the following formula:

$$ECV_{(d_b),(F),(e),(i)} = \overline{CV}_{high} - \overline{CV}_{low} \tag{3}$$

After effects calculation, Pareto analysis technique is used to sort the regime parameters, according to their levels of significance (see Fig. 5, a, c).

a)

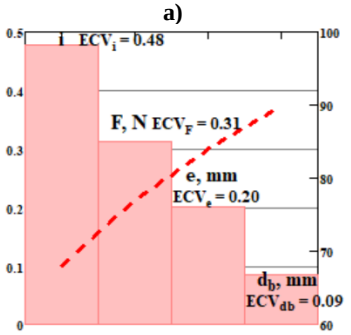

b)

ANOVA =

"Source"	"SSE"	"DF"	"MSE"	"F-statistic"	"P-statistic"
"db,mm"	0.467	1.000	0.467	0.185	0.669
"F,N"	6.256	1.000	6.256	2.480	0.121
"e, mm"	2.607	1.000	2.607	1.033	0.314
"i"	14.576	1.000	14.576	5.778	0.019
"Error"	148.851	59.000	2.523	NaN	NaN
"Total"	172.757	63.000	NaN	NaN	NaN

c)

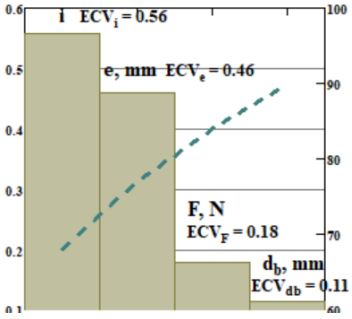

d)

ANOVA =

"Source"	"SSE"	"DF"	"MSE"	"F-statistic"	"P-statistic"
"db,mm"	0.828	1.000	0.828	0.294	0.590
"F,N"	2.030	1.000	2.030	0.720	0.400
"e, mm"	13.452	1.000	13.452	4.771	0.033
"i"	19.872	1.000	19.872	7.048	0.010
"Error"	166.357	59.000	2.820	NaN	NaN
"Total"	202.539	63.000	NaN	NaN	NaN

Fig. 5. a, c) Pareto histograms for the influence of the BB's regime parameters on RR's cells parameters Dc and δ; b, d) ANOVA results for determining the significantly influenced BB's regime parameters over RR's cells parameters Dc and δ.

Two ANOVA studies [24] also are conducted to determine the F-statistic values of the BB regime parameters (see Fig. 5, b, d). For the accepted 95%

confidence level and total degrees of freedom $DF = (Runs \cdot Repplications) - 1 = (16 \cdot 4) - 1 = 63$, the critical Fisher value is 3.993.

4. Results and discussion

As can be seen from Table 2, the diameter of the inscribed circle Dc has the minimum CV = 0.936% (see row 7, column 4 from Table 2), and it is obtained with combination of burnishing parameters: *dc*= 6 mm, *F*= 380 N, *e*= 1.0 mm, and *i*= 1650.15. The maximum value of CV reaches 7.15% (see row 5, column 2 from Table 2) in regime parameter combination values: *dc*= 6 mm, *F*= 380 N, *e*= 0.5 mm, and *i*= 1650.15.

The calculated effects of the BB's regime parameters on RR's cells size variability (see Fig. 5, a) show that maximum effect is caused by parameter *i*, followed by parameters *F*, N. The conducted ANOVA analysis and the obtained F-statistic values (see Fig. 5, b), however, show that only parameter *i* is statistically significant because the F-value = 5.778 is greater than the calculated critical Fisher value, which in this case is 3.993.

Analyzing the coefficients of variation of the angle δ, it is seen that the lowest CV value is 0.356% (see row 2, column 5 from Table 2) and the maximum CV value is 7.832 % (see row 16, column 6 from Table 2). They are obtained respectively with combination of the regime parameters: for minimum CV: d_b= 6 mm, *F*= 250 N, *e*= 0.5 mm, and *i*= 2500.15, and for maximum CV: d_b= 8 mm, *F*= 380 N, *e*= 1.0 mm, and *i*= 2500.15.

The Pareto histogram (see Fig. 5, c) shows that the parameters *i* and *e* have significant effects on the variability of the RR's cells shape. As can be seen from this figure (Fig. 5, c), larger CV values are obtained at the higher levels of these two regime parameters. The F-statistic values of the BB's regime parameters *i* (7.048) and *e* (4.771) (see Fig. 5, d) confirm this hypothesis, because they are greater than the critical Fisher value (3.993).

6. Conclusions

Based on the conducted experimental studies and the obtained results, the following conclusions can be drawn:

- The finishing operation for obtaining RR on complex functional surfaces by simultaneous five-axis BB, performed on multi-axis CNC milling center achieves the intended goal. In all combinations of low and high values of the BB regime parameters, fully RR of the IV^{-th} type is successfully formed onto complex surfaces.
- Despite of the general similarity of the obtained results in the current work and in source [22], the herein proposed measuring setup (see Fig. 4, a) for determining the RR' cells parameters: angle δ, and the diameter of the inscribed circle Dc, can assure greater accuracy.

- Using the coefficient of variance CV for expressing the obtained cells shape and size variability, significantly reduces the experimental data and provides a quicker and easier way to their interpretation.
- The RR's cells formed can be considered as sufficiently homogeneous with a maximum variability of up to 8% in terms of their size and shape, although they are processed onto complex spatial surface, using projected planar toolpath polyline.
- Of the four main burnishing parameters studied, the variability of RR's cells size and shape is more significantly influenced by parameters *i* and *e*, which are related to the geometrical characteristics of the deforming element toolpath than the other two parameters (d_b and F), which refer to the plastic deformation in the surface layer.
- In addition to the investigated aluminum specimens, RR may be formed by using a multi-axis BB operation onto complex surfaces of workpieces, made of higher hardness materials (such as steel, polymers, other nonferrous materials, etc.). This will not automatically lead to a significant increase in the deforming force, because despite the needed complex spatial toolpath of the deforming tool, due to the multi-axis CNC machines high precision and repeatability, a multi-pass burnishing operation can be carried out, without risking to disrupt the already formed RR's cells during the previous pass.

The results, obtained from current experimental study can be used in future optimization studies to obtain RR's cells of an optimal size and shape, in accordance with the operational requirements of a similar type of functional surface, of the type shown on Fig. 3, d.

REFERENCES

[1]. *L. G. Odintsov*, Hardening and Finishing of Parts by Surface Plastic Deformation, Mashinostroenie, Moscow, 1987.
[2]. *R. Horváth, Drégelyi-Kiss Ágota, M. Gyula*, The examination of surface roughness parameters in the fine turning of Hypereutectic aluminium alloys, Scientific Bulletin-University Politehnica of Bucharest Series D 77, no. 2 (2015): 205-216.
[3]. *N. Neacsu*, Reaming with diamond and cubic boron nitride abrasive, University "Politehnica" of Bucharest Scientific Bulletin, Series D: Mechanical Engineering 64, no. 3 (2002): 25-34.
[4]. *Yu. G. Schneider*, Operational properties of parts with regular microrelief, publishing IVA, St. Petersburg, ISBN 5-7577-0166-8, 2001.
[5]. "ECOROLL AG Catalog," ECOROLL AG Werkzeugtechnik, 2020. [Online]. Available: https://www.ecoroll.de/en/service/downloads.html . [Accessed 14 January 2020].
[6]. "Cogsdill Burnishing Tools" Cogsdill Tool Products, Inc., [En ligne]. Available: https://cogsdill.com/products/burnishing-tools/ . [Accessed 14 January 2020].
[7]. Y. *S. Feldman et A. N. Kravtsov*, Proficorder study of vibratory ball-burnished surfaces, Measurement Techniques, vol. 12, n° 112, pp. 1789-1790, 1969.
[8]. *R. Jerez-Mesa, J.A. Travieso-Rodríguez, Y. Landon, G. Dessein, J. Lluma-Fuentes, V. Wagner*, Comprehensive analysis of surface integrity modification of ball-end milled Ti-6Al-4V surfaces

through vibration-assisted ball burnishing. Journal of Materials Processing Technology. 2019 May 1;267: 230-240.

[9].*G. Nagîţ, L. Slătineanu, O. Dodun, M.I. Rîpanu, A.M. Mihalache*, Surface layer microhardness and roughness after applying a vibroburnishing process. Journal of Materials Research and Technology, 8(5), 2019, pp.4333-4346.

[10]. *G. Nagîţ, O. Dodun, L. Slătineanu, M.I. Rîpanu*, Behavior of some steels at vibrorolling, MATEC Web of Conferences 121, p. 03016, 2017.

[11]. A.P. Sebe, C. Minciu, Stage Specifical Approach In NC Milling Of Geometrically-Complex Surfaces. University" Politehnica" of Bucharest Scientific Bulletin, Series D: Mechanical Engineering. 2004;66(2):9-20.

[12]. *L. N. López de Lacalle, A. Rodriguez, A. Lamikiz, A. Celaya, R. Alberdi*, Five-axis machining and burnishing of complex parts for the improvement of surface roughness. Materials and Manufacturing Processes. 2011 Aug 1;26(8):997-1003.

[13]. *E. Bachtiak-Radka, S. Dudzińska, D. Grochała, S. Berczyński, W. Olszak*. The influence of CNC milling and ball burnishing on shaping complex 3D surfaces. Surface Topography: Metrology and Properties. 2017 Jan 27, 5(1):015001.

[14]. *S. Slavov*, An Algorithm for Generating Optimal Toolpaths for CNC Based Ball-Burnishing Process of Planar Surfaces, In International Conference on Intelligent Information Technologies for Industry, pp. 365-375. Springer, Cham, 2017.

[15]. *H. Basak, M.T. Ozkan, I. Toktas*, Experimental research and ANN modeling on the impact of the ball burnishing process on the mechanical properties of 5083 Al-Mg material. Kovove Mater. 2019 Jan 1; 57: 61-74.

[16]. *A. Dzierwa, A. P. Markopoulos*, Influence of Ball-Burnishing Process on Surface Topography Parameters and Tribological Properties of Hardened Steel. Machines. 2019 Mar;7(1):11.

[17]. *F. Gharbi, S. Sghaier, F. Morel, T. Benameur*. Experimental investigation of the effect of burnishing force on service properties of AISI 1010 steel plates. Journal of Materials Engineering and Performance. 2015 Feb 1;24(2):721-725.

[18]. *F.J. Shiou, C.H. Chen*. Freeform surface finish of plastic injection mold by using ball-burnishing process. Journal of Materials Processing Technology. 2003 Sep 22;140(1-3):248-254.

[19]. *Ts. Kaldashev, P. Hadjiiski*, Study of Error Establishment in Milling Machines with 5 Axes, In Proceedings of the 12th International Scientific and Practical Conference. Volume III, vol. 81, p. 83. 2019.

[20]. *Ts. Kaldashev*, Method for Measuring Error Establishment in 5-Axis Milling Machines with a Touch Probe, In Proceedings of the 12th International Scientific and Practical Conference. Volume III, vol. 77, p. 80. 2019.

[21]. *K. Apro*, Secrets of 5-axis machining. Industrial Press Inc.; 2008, ISBN 978-0-8311-3375-7.

[22]. *I. Iliev*, Research on the influence of the five-axis ball-burnishing process regime parameters on the resulted cells properties from regularly shaped roughness, Annual Journal of Technical University of Varna, Bulgaria, vol. 3, no. 1, pp. 40-53, Jun. 2019.

[23]. *S. Slavov, I. Iliev*, Design and FEM static analysis of an instrument for surface plastic deformation of non-planar functional surfaces of machine parts, Fiability & Durability, ISSN 1844 – 640X, 2016, Nov 1(2).

[24]. *D.C. Montgomery*, Design and analysis of experiments, John Wiley & Sons, 2017.

[25]. *M. H. Kutner, J. Neter, C. J. Nachtsheim, W. Li*, Applied Linear Statistical Models, 5th ed., McGraw-Hill Education, 2004.